European Journal of
Mineralogy
Open Access

Supplement of

Fe^{3+}/ΣFe variation in lawsonite and epidote in subducted oceanic crust

Donna L. Whitney et al.

Correspondence to: Donna L. Whitney (dwhitney@umn.edu)

Supplementary material

1. XANES analytical procedures and modeling

XANES analyses were acquired with two Silicon (311) monochromator crystals that provide an energy resolution of $\Delta E/E = 2.8 \times 10^{-5}$. At 7000 eV, this corresponds to an energy resolution of 0.196 eV. Each scan was ~10 minutes in duration, with 1 second/point acquisition. The original, non-averaged data are provided in Table S1.

After normalization of the XANES spectrum, several eV below and above the pre-edge were used to model the background by the main edge to this region. This was done using the limb of a Lorentzian. This function was subtracted from the normalized spectrum, yielding the pre-edge (Fig. 1b). The background subtracted spectrum was directly used to numerically determine the centroid energy and intensity. No peaks were fitted to the pre-edge itself. This procedure was first used by Wilke et al. (2009) and yielded reliable results. It avoids fits with many parameters and a choice of line form for the pre-edge peaks. We used scripts programmed in Igor Pro for processing.

Regarding uncertainties: $Fe^{3+}/Fe > Fe$ is a result of orientation effects that skew the relation between the centroid and oxidation state. The calibration assumes that all electronic transitions are excited equally, as in a randomly oriented powder. The linear dichroism breaks this assumption by exciting some transitions preferentially at a given crystal orientation. This leads to overestimation or underestimation of the "normal" centroid value. Calculation of the oxidation state may (for example) result in values between 0.8 and 1.2 for a true value of 1.0 (e.g., in the case of epidote). For the other minerals measured in this study, the effect is smaller to negligible, as discussed in the text.

The uncertainties provided are estimated based on the reproducibility of the analysis of the centroid. The uncertainty in centroid energy has been propagated to oxidation state using the polynomial with the uncertainty of the parameters given. Uncertainties are standard deviations. The estimated uncertainties are within the energy resolution provided from the beamline setting.

Table S1: XANES data (ESRF, BM23, April 2023)

| | | | calibrations | |
| | | | old | new |
reference materials	centroid	intensity	Fe3+/ΣFe	Fe3+/ΣFe
olivine_scan3	7111.96	0.0695	-0.02	**-0.01**
olivine_scan6	7112.01	0.0704	0.00	**0.01**
olivine_scan6	7112.00	0.0710	0.00	**0.00**
olivine_scan9	7111.99	0.0714	-0.01	**0.00**
olivine_scan12	7112.00	0.0698	0.00	**0.00**
acmite_scan17	7113.65	0.0763	1.19	**1.04**

acmite_scan17	7113.64	0.0809	1.17	**1.03**
acmite_1_scan17	7113.66	0.0759	1.20	**1.05**
acmite_2_scan3	7113.80	0.0924	1.42	**1.16**
andradite_scan3	7113.61	0.0668	1.14	**1.00**
siderite_scan3	7112.00	0.0958	0.00	**0.00**
sancarlos_scan3	7111.95	0.0601	-0.03	**-0.02**
pjo92190_scan7	7112.98	0.0818	0.57	**0.54**
pjo92190_scan10	7112.95	0.0808	0.55	**0.52**
pjo92190_scan13	7112.90	0.0793	0.52	**0.49**
pjo92190_scan16	7113.00	0.0804	0.59	**0.55**
pjo92190_scan22	7112.82	0.0683	0.47	**0.44**
pjo92190_scan25	7112.88	0.0679	0.50	**0.48**
NC18_08A_alm_Saggrenda_scan4	7112.04	0.0761	0.02	**0.02**
NC18_08A_alm_Saggrenda_scan7	7112.04	0.0778	0.02	**0.02**
lawsonite grain mount (Franciscan/ UMN)				
UMNlws_xtal3_scan3	7113.65	0.0606	1.19	**1.04**
UMNlws_xtal3_scan10	7113.66	0.0623	1.21	**1.05**
UMNlws_xtal3_scan13	7113.76	0.0643	1.35	**1.13**
UMNlws_xtal3_scan16	7113.69	0.0600	1.24	**1.07**
UMNlws_xtal3_scan19	7113.66	0.0624	1.20	**1.05**
UMNlws_xtal3_scan22	7113.76	0.0592	1.36	**1.13**
UMNlws_xtal3_scan25	7113.60	0.0652	1.13	**1.00**
UMNlws_xtal3_scan28	7113.64	0.0616	1.17	**1.03**
UMNlws_xtal3_scan31	7113.60	0.0645	1.13	**1.00**
UMNlws_xtal3_scan34	7113.59	0.0666	1.11	**0.99**
UMNlws_xtal3_scan37	7113.65	0.0639	1.19	**1.04**
UMNlws_xtal3_scan40	7113.65	0.0604	1.20	**1.04**
UMNlws_xtal3_scan43	7113.67	0.0620	1.21	**1.05**
UMNlws_xtal3_scan46	7113.65	0.0595	1.20	**1.04**
UMNlws_xtal2_scan49	7113.54	0.0667	1.05	**0.95**
UMNlws_xtal2_scan52	7113.66	0.0641	1.20	**1.05**
UMNlws_xtal2_scan55	7113.70	0.0650	1.25	**1.08**
UMNlws_xtal2_scan58	7113.63	0.0600	1.17	**1.02**
UMNlws_xtal2_scan61	7113.65	0.0616	1.18	**1.04**
UMNlws_xtal2_scan64	7113.68	0.0616	1.23	**1.06**
UMNlws_xtal2_scan67	7113.68	0.0611	1.23	**1.06**
UMNlws_xtal2_scan70	7113.65	0.0612	1.19	**1.04**
UMNlws_xtal2_scan73	7113.68	0.0628	1.23	**1.06**
UMNlws_xtal2_scan76	7113.66	0.0588	1.20	**1.05**
UMNlws_xtal2_scan79	7113.73	0.0611	1.30	**1.10**
UMNlws_xtal2_scan82	7113.75	0.0593	1.33	**1.12**
UMNlws_xtal2_scan85	7113.66	0.0628	1.21	**1.05**
UMNlws_xtal2_scan88	7113.77	0.0607	1.37	**1.14**
UMNlws_xtal2_scan91	7113.68	0.0596	1.23	**1.06**
UMNlws_xtal2_scan94	7113.68	0.0587	1.23	**1.06**
UMNlws_xtal2_scan97	7113.69	0.0635	1.24	**1.07**

UMNlws_xtal2_scan100	7113.62	0.0611	1.16	**1.01**
UMNlws_xtal2_scan103	7113.71	0.0610	1.28	**1.09**
UMNlws_xtal2_scan106	7113.69	0.0625	1.24	**1.07**
UMNlws_xtal2_scan109	7113.72	0.0613	1.29	**1.10**
UMNlws_xtal2_scan112	7113.75	0.0586	1.33	**1.12**
lawsonite in eclogite thin section (Sivrihisar, Turkey); not shown: garnet data				
SV12_13D1_scan3	7113.80	0.0538	1.42	**1.16**
SV12_13D1_scan6	7113.80	0.0568	1.42	**1.16**
SV12_13D1_scan16	7113.30	0.0612	0.82	**0.76**
SV12_13D1_scan19	7113.75	0.0610	1.33	**1.12**
SV12_13D1_scan22	7113.73	0.0569	1.30	**1.10**
SV12_13D1_scan36	7113.68	0.0686	1.24	**1.06**
SV12_13D1_scan39	7113.32	0.0570	0.84	**0.78**
SV12_13D1_scan42	7113.38	0.0601	0.89	**0.82**
SV12_13D1_scan46	7113.58	0.0600	1.11	**0.98**
SV12_13D1_scan49	7113.56	0.0638	1.08	**0.96**
SV12_13D1_scan52	7113.56	0.0687	1.08	**0.96**
SV12_13D1_scan55	7113.54	0.0645	1.05	**0.95**
SV12_13D1_scan69	7113.61	0.0602	1.13	**1.00**
SV12_13D1_scan72	7113.59	0.0627	1.12	**0.99**
SV12_13D1_scan75	7113.68	0.0573	1.23	**1.06**
SV12_13D1_scan78	7113.68	0.0604	1.23	**1.06**
SV12_13D1_scan81	7113.65	0.0587	1.19	**1.04**
SV12_13D1_scan84	7113.55	0.0630	1.07	**0.96**
SV12_13D1_scan87	7113.57	0.0695	1.09	**0.97**
SV12_13D1_scan90	7113.61	0.0619	1.13	**1.00**
SV12_13D1_scan93	7113.54	0.0680	1.06	**0.95**
SV12_13D1_scan96	7113.60	0.0662	1.12	**1.00**
SV12_13D1_scan99	7113.56	0.0629	1.08	**0.96**
SV12_13D1_scan102	7113.60	0.0631	1.13	**1.00**
SV12_13D1_scan105	7113.61	0.0640	1.14	**1.00**
SV12_13D1_scan108	7113.46	0.0718	0.97	**0.89**
SV12_13D1_scan111	7113.53	0.0643	1.05	**0.94**
SV12_13D1_scan114	7113.51	0.0663	1.03	**0.92**
SV12_13D1_scan117	7113.51	0.0646	1.03	**0.92**
SV12_13D1_scan120	7113.45	0.0650	0.97	**0.88**
SV12_13D1_scan150	7113.35	0.0651	0.87	**0.80**
SV12_13D1_scan153	7113.39	0.0563	0.91	**0.83**
SV12_13D1_scan156	7113.44	0.0593	0.95	**0.87**
SV12_13D1_scan159	7113.44	0.0628	0.95	**0.87**
SV12_13D1_scan162	7113.40	0.0625	0.91	**0.84**
SV12_13D1_scan177	7113.42	0.0836	0.93	**0.85**
SV12_13D1_scan180	7113.50	0.0679	1.01	**0.92**
SV12_13D1_scan183	7113.45	0.0652	0.96	**0.88**

SV12_13D1_scan186	7113.48	0.0685	0.99	**0.90**	
SV12_13D1_scan189	7113.56	0.0650	1.08	**0.96**	

lawsonite in blueschist thin sections (New Caledonia)

NC19_159_scan6	7112.84	0.0681	0.48	**0.45**	rim
NC19_159_scan9	7112.91	0.0882	0.52	**0.49**	rim
NC19_159_scan12	7112.99	0.0637	0.58	**0.55**	core
NC19_159_scan15	7113.21	0.0669	0.75	**0.70**	rim
NC19_159_scan18	7113.14	0.0692	0.69	**0.65**	core
NC19_159_scan21	7113.02	0.0561	0.60	**0.57**	core
NC19_159_scan24	7112.93	0.0707	0.54	**0.51**	rim
NC19_159_scan27	7113.02	0.0647	0.60	**0.57**	rim
NC19_159_scan30	7113.04	0.0654	0.62	**0.58**	rim
NC19_159_scan35	7113.16	0.0617	0.70	**0.66**	core
NC19_159_scan38	7113.18	0.0601	0.73	**0.68**	core
NC19_159_scan41	7113.09	0.0582	0.65	**0.61**	core
NC19_159_scan44	7113.17	0.0630	0.71	**0.67**	rim
NC19_159_scan48	7112.98	0.0620	0.57	**0.54**	rim
NC19_159_scan53	7112.54	0.0603	0.29	**0.27**	core
NC19_159_scan56	7112.82	0.0593	0.47	**0.44**	
NC19_159_scan59	7113.02	0.0683	0.60	**0.57**	rim

note: scans 12, 18, 21 = same pt; scans 15, 24, 27, 30 = same pt

NC18_01_xtal1_scan4	7112.86	0.0550	0.49	**0.46**	
NC18_02_xtal1_scan17	7113.01	0.0620	0.59	**0.56**	
NC18_01_xtal2_scan20	7112.96	0.0634	0.56	**0.53**	
NC18_01_xtal2_scan23	7113.02	0.0669	0.60	**0.57**	rim
NC18_01_xtal2_scan26	7113.07	0.0605	0.64	**0.60**	
NC18_01_xtal3_scan29	7113.26	0.0687	0.79	**0.74**	rim
NC18_01_xtal3_scan32	7113.19	0.0609	0.73	**0.68**	
NC18_01_xtal4_scan53	7112.70	0.0583	0.39	**0.36**	rim
NC18_01_xtal4_scan56	7112.69	0.0640	0.38	**0.36**	
NC18_01_xtal5_scan59	7112.85	0.0615	0.49	**0.46**	core
NC18_01_xtal5_scan62	7112.74	0.0540	0.42	**0.39**	
NC18_01_xtal5_scan65	7113.00	0.0582	0.59	**0.55**	rim
NC18_01_xtal5_scan68	7112.92	0.0609	0.53	**0.50**	
NC18_01_xtal6_scan71	7112.68	0.0492	0.38	**0.35**	rim
NC18_01_xtal6_scan74	7112.45	0.0470	0.24	**0.22**	
NC18_01_xtal6_scan77	7112.99	0.0642	0.58	**0.55**	mid
NC18_01_xtal6_scan80	7112.98	0.0651	0.58	**0.54**	
NC18_01_xtal6_scan83	7112.81	0.0641	0.46	**0.43**	core
NC18_01_xtal6_scan86	7112.85	0.0600	0.49	**0.46**	
NC18_01_xtal7_scan89	7112.94	0.0689	0.54	**0.51**	rim
NC18_01_xtal7_scan92	7113.03	0.0628	0.61	**0.57**	
NC18_01_xtal7_scan95	7112.96	0.0582	0.56	**0.53**	mid
NC18_01_xtal7_scan98	7113.03	0.0605	0.61	**0.57**	
NC18_01_xtal7_scan101	7112.71	0.0555	0.39	**0.37**	core

NC18_01_xtal7_scan104	7112.71	0.0606	0.40	**0.37**

epidote grain mount (Bayreuth)

epidote_bt_scan6	7113.82	0.0897	1.46	**1.18**
epidote_bt_scan9	7113.80	0.0893	1.43	**1.16**
epidote_bt_scan12	7113.81	0.0881	1.45	**1.17**
epidote_bt_scan16	7113.57	0.0942	1.10	**0.97**
epidote_bt_scan19	7113.57	0.0881	1.09	**0.97**
epidote_bt_scan23	7113.60	0.0715	1.12	**1.00**
epidote_bt_scan26	7113.58	0.0738	1.11	**0.98**

clinozoisite grain mount (Gilgit, Pakistan)

clz_pakistan_scan9	7113.93	0.0796	1.88	**1.28**
clz_pakistan_scan12	7113.92	0.0851	1.77	**1.27**
clz_pakistan_scan20	7113.51	0.0909	1.03	**0.92**
clz_pakistan_scan23	7113.49	0.0887	1.00	**0.91**
clz_pakistan_scan27	7113.71	0.1134	1.28	**1.09**
clz_pakistan_scan30	7113.68	0.1141	1.24	**1.06**

EGMs in blueschist/eclogite thin sections (New Caledonia)

NC19_43_scan5	7113.55	0.0803	1.07	**0.96**
NC19_43_scan11	7113.54	0.0790	1.06	**0.95**
NC19_43_scan18	7113.57	0.0802	1.09	**0.97**
NC19_43_scan21	7113.59	0.0798	1.12	**0.99**
NC19_43_scan24	7113.07	0.0744	0.64	**0.60**
NC19_43_scan27	7113.10	0.0743	0.66	**0.62**
NC19_43_scan30	7113.13	0.0725	0.68	**0.64**
NC19_43_scan33	7113.13	0.0749	0.68	**0.64**
NC19_43_scan36	7113.63	0.0849	1.16	**1.02**
NC19_43_scan39	7113.58	0.0856	1.10	**0.98**
NC19_43_scan43	7113.53	0.0988	1.04	**0.94**
NC19_43_scan46	7113.52	0.0977	1.03	**0.93**
NC19_43_scan51	7113.44	0.0836	0.95	**0.87**
NC19_43_scan54	7113.46	0.0805	0.98	**0.89**
NC19_43_scan70	7113.35	0.0750	0.86	**0.80**
NC19_43_scan73	7113.32	0.0770	0.84	**0.78**
NC18_30B_scan9	7113.69	0.1012	1.25	**1.07**
NC18_30B_scan12	7113.69	0.1105	1.25	**1.07**
NC18_30B_scan15	7113.75	0.0710	1.33	**1.12**
NC18_30B_scan18	7113.75	0.0722	1.34	**1.12**
NC18_30B_scan21	7113.75	0.0829	1.34	**1.12**
NC18_30B_scan24	7113.73	0.0822	1.30	**1.10**
NC18_30B_scan27	7113.72	0.0783	1.28	**1.10**
NC18_30B_scan30	7113.75	0.0775	1.33	**1.12**
NC18_30B_scan33	7113.58	0.1094	1.10	**0.98**
NC18_30B_scan36	7113.58	0.1101	1.10	**0.98**

NC18_30B_scan57	7113.45	0.1179	0.96	**0.88**
NC18_08A_scan4	7113.49	0.0916	1.01	**0.91**
NC18_08A_scan7	7113.50	0.0958	1.02	**0.92**
NC18_08A_scan10	7113.44	0.1099	0.95	**0.87**
NC18_08A_scan13	7113.42	0.1095	0.93	**0.85**
NC18_08A_scan16	7113.46	0.1088	0.97	**0.89**
NC18_08A_scan19	7113.46	0.1084	0.98	**0.89**
NC18_08A_scan22	7113.51	0.1099	1.02	**0.92**
NC18_08A_scan25	7113.49	0.1099	1.00	**0.91**
NC18_08A_scan28	7113.51	0.1124	1.02	**0.92**
NC18_08A_scan31	7113.50	0.1118	1.01	**0.92**
NC18_08A_scan34	7113.41	0.1160	0.92	**0.85**
NC18_08A_scan37	7113.41	0.1142	0.93	**0.85**
NC18_08A_scan40	7113.70	0.0785	1.26	**1.08**
NC18_08A_scan43	7113.71	0.0757	1.28	**1.09**
NC18_08A_scan46	7113.73	0.0799	1.31	**1.10**
NC18_08A_scan49	7113.75	0.0765	1.33	**1.12**
NC18_08A_scan52	7113.62	0.0839	1.15	**1.01**
NC18_08A_scan55	7113.61	0.0855	1.14	**1.00**
NC18_08A_scan58	7113.61	0.0891	1.13	**1.00**
NC18_08A_scan61	7113.63	0.0861	1.16	**1.02**
NC18_08A_scan64	7113.38	0.0855	0.90	**0.82**
NC18_08A_scan67	7113.39	0.0850	0.91	**0.83**
NC18_08A_2_scan3	7113.39	0.0959	0.90	**0.83**
NC18_08A_2_scan6	7113.39	0.0943	0.90	**0.83**
NC18_08A_2_scan9	7113.37	0.1157	0.89	**0.82**
NC18_08A_2_scan12	7113.37	0.1140	0.88	**0.82**
lawsonite grain mount (Franciscan / Smithsonian)				
Lws_smithsonian_xtal1_scan3	7113.57	0.0609	1.09	**0.97**
Lws_smithsonian_xtal1_scan6	7113.63	0.0643	1.17	**1.02**
Lws_smithsonian_xtal1_scan9	7113.58	0.0610	1.11	**0.98**
Lws_smithsonian_xtal1_scan12	7113.69	0.0578	1.25	**1.07**
Lws_smithsonian_xtal2_scan3	7113.53	0.0584	1.05	**0.94**
Lws_smithsonian_xtal2_scan6	7113.52	0.0570	1.03	**0.93**
Lws_smithsonian_xtal2_scan9	7113.57	0.0571	1.09	**0.97**
Lws_smithsonian_xtal2_scan12	7113.54	0.0566	1.06	**0.95**
Lws_smithsonian_xtal3_scan3	7113.52	0.0551	1.03	**0.93**
Lws_smithsonian_xtal3_scan6	7113.46	0.0564	0.97	**0.89**
Lws_smithsonian_xtal3_scan9	7113.50	0.0547	1.01	**0.92**
Lws_smithsonian_xtal3_scan12	7113.49	0.0547	1.00	**0.91**
zoisite grain mount (loc. unknown / UMN)				
UMN_Zo_xtal1_scan3	7113.34	0.0662	0.86	**0.79**
UMN_Zo_xtal1_scan6	7113.31	0.0666	0.83	**0.77**

UMN_Zo_xtal2_scan3	7112.95	0.0724	0.55	**0.52**
UMN_Zo_xtal2_scan6	7112.96	0.0683	0.56	**0.53**
UMN_Zo_xtal2_scan9	7113.00	0.0730	0.58	**0.55**
UMN_Zo_xtal3_scan3	7113.49	0.0748	1.00	**0.91**
UMN_Zo_xtal3_scan6	7113.46	0.0759	0.97	**0.89**
UMN_Zo_xtal3_scan9	7113.52	0.0721	1.04	**0.93**
UMN_Zo_xtal4_scan3	7112.99	0.0709	0.58	**0.55**
UMN_Zo_xtal4_scan6	7112.96	0.0694	0.56	**0.53**
UMN_Zo_xtal4_scan9	7113.01	0.0747	0.60	**0.56**

lawsonite mineral separate from blueschist (Corsica)				
Lws_corsica_scan6	7113.48	0.0730	0.99	**0.90**
Lws_corsica_xtal3_scan18	7113.76	0.0560	1.35	**1.13**
Lws_corsica_xtal1b_scan3	7113.48	0.0552	0.99	**0.90**
Lws_corsica_xtal1b_scan6	7113.59	0.0732	1.12	**0.99**
Lws_corsica_xtal1b_scan9	7113.70	0.0534	1.26	**1.08**
Lws_corsica_xtal1b_scan12	7113.73	0.0569	1.30	**1.10**
Lws_corsica_xtal1b_scan15	7113.72	0.0582	1.29	**1.10**
Lws_corsica_xtal1b_scan18	7113.59	0.0621	1.11	**0.99**
Lws_corsica_xtal1b_scan21	7113.57	0.0676	1.09	**0.97**
Lws_corsica_xtal1b_scan24	7113.76	0.0511	1.35	**1.13**
Lws_corsica_xtal1b_scan27	7113.60	0.0507	1.13	**1.00**
Lws_corsica_xtal1b_scan30	7113.72	0.0682	1.29	**1.10**
Lws_corsica_xtal1b_scan33	7113.55	0.0677	1.07	**0.96**
Lws_corsica_xtal1b_scan36	7113.75	0.0600	1.34	**1.12**
Lws_corsica_xtal1b_scan39	7113.71	0.0705	1.27	**1.09**
Lws_corsica_xtal1b_scan42	7113.91	0.0595	1.71	**1.26**
Lws_corsica_xtal1b_scan45	7113.75	0.0669	1.33	**1.12**
Lws_corsica_xtal1b_scan48	7113.81	0.0555	1.44	**1.17**
Lws_corsica_xtal1b_scan51	7113.72	0.0549	1.29	**1.10**
Lws_corsica_xtal1b_scan54	7113.55	0.0635	1.07	**0.96**
Lws_corsica_xtal1b_scan57	7113.57	0.0566	1.09	**0.97**
Lws_corsica_xtal1b_scan63	7113.66	0.0659	1.21	**1.05**
Lws_corsica_xtal1b_scan66	7113.77	0.0607	1.37	**1.14**
Lws_corsica_xtal1b_scan69	7113.64	0.0663	1.17	**1.03**
Lws_corsica_xtal1b_scan72	7113.49	0.0605	1.00	**0.91**
Lws_corsica_xtal1b_scan75	7113.69	0.0658	1.25	**1.07**
Lws_corsica_xtal1b_scan78	7113.72	0.0618	1.29	**1.10**
Lws_corsica_xtal1b_scan81	7113.73	0.0679	1.30	**1.10**
Lws_corsica_xtal1b_scan84	7113.87	0.0518	1.57	**1.22**
Lws_corsica_xtal1b_scan87	7113.83	0.0555	1.49	**1.19**
Lws_corsica_xtal1b_scan90	7113.80	0.0616	1.43	**1.16**
Lws_corsica_xtal1b_scan96	7113.72	0.0613	1.29	**1.10**
Lws_corsica_xtal1b_scan99	7113.72	0.0615	1.29	**1.10**
Lws_corsica_xtal1b_scan102	7113.81	0.0553	1.45	**1.17**
Lws_corsica_xtal1b_scan105	7113.54	0.0620	1.06	**0.95**
Lws_corsica_xtal1b_scan108	7113.80	0.0654	1.43	**1.16**

Lws_corsica_xtal1b_scan111	7113.82	0.0537	1.45	**1.18**
Lws_corsica_xtal1b_scan114	7113.56	0.0568	1.08	**0.96**

Figure S1: Additional XANES spectra for zoisite and clinozoisite. For each, a large single crystal was cut along distinct planes and analysed as a grain mount. (a) Spectra and grain mount images for zoisite from the University of Minnesota collection (locality unknown); (b) Spectra and grain mount image for clinozoisite from Gilgit, Pakistan. Numbers on grain mount correspond to grains/crystals (Table S1).
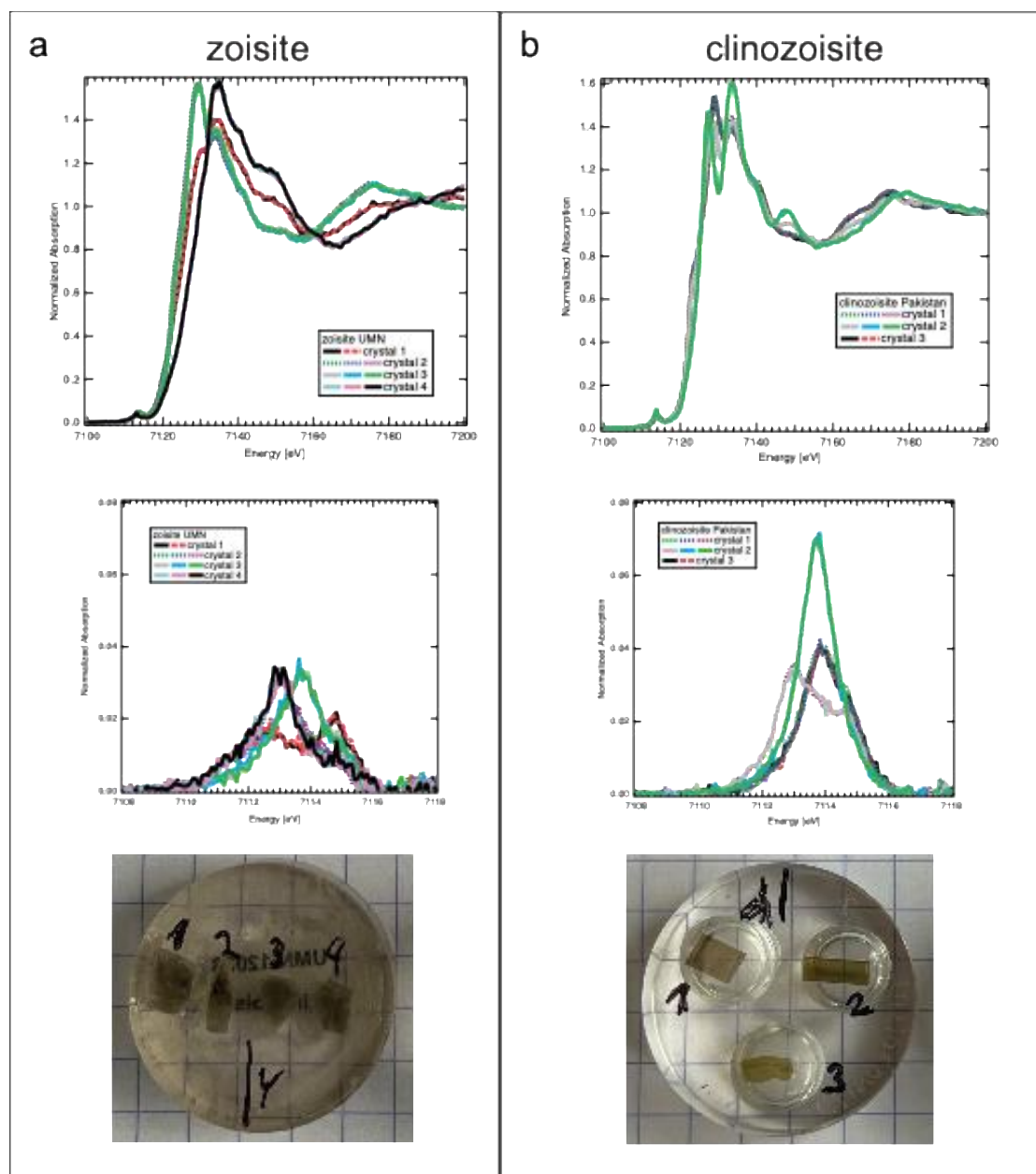
Figure S2: Normalized XANES (red) spectra of reference minerals analysed in this study. Markers indicate the regions of the spectra that were taken for fitting the background with a Lorentzian. Black lines show fitted function, which was subtracted from the normalized XANES. Spectra are offset for clarity.
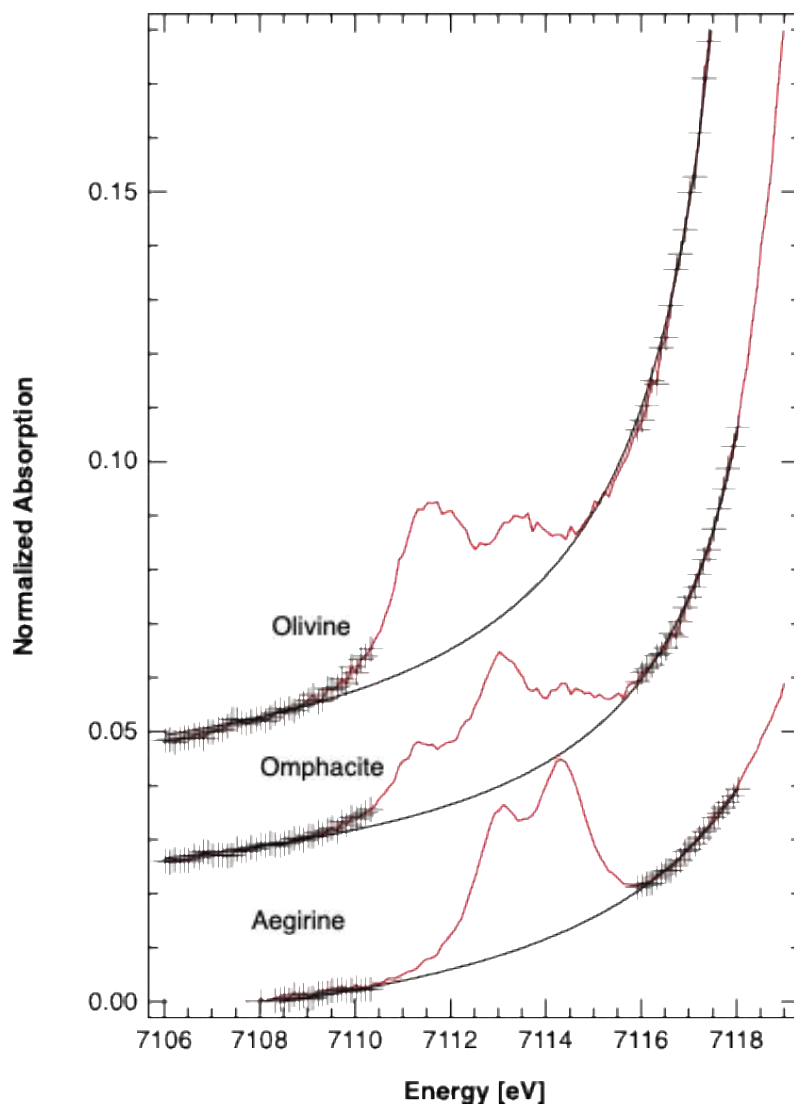
2. EPMA methods and results (mineral composition data)

Lawsonite and EGM compositions and element maps were collected using the JEOL JXA-8530FPlus Electron Probe Microanalyzer in the Department of Earth and Environmental Sciences at the University of Minnesota and using the JEOL JXA-8200 in the Institut für Geowissenschaften at Universität Potsdam. At UMN, quantitative analyses were conducted using a 20 kV accelerating voltage, 20 nA beam current, and a defocused beam (5 μm). At Potsdam, analyses were acquired using a 15 kV accelerating voltage, 15 nA beam current, and a defocused beam (5 μm). Standards included natural and synthetic minerals. Correction methods included ZAF and Phi-Rho-Z. Element maps (Fig. 3g, h) were collected using a 50 nA beam current.

Table S2a: EPMA data: representative compositions for lawsonite analysed by XANES.

mineral	Lws	Lws	Lws	Lws	Lws	Lws	Lws	Lws
locality	Franciscan USA	Franciscan USA	Sivrihisar Turkey	New Cal.	New Cal.	New Cal.	New Cal.	New Cal.
sample	Smiths. grain 1	UMN grain 1	SV12-13D	NC19-159	NC18-01	NC18-01	NC18-01	NC18-01
EPMA	UMN	UMN	Potsdam	Potsdam	UMN	UMN	UMN	UMN
type/pt	*GM*	*GM*	*TS*	*TS*	*TS-pt 1*	*pt 2*	*pt 3*	*pt 4*
SiO_2	38.73	37.52	38.16	38.33	38.11	38.27	38.37	38.38
TiO_2	0.14	0.84	0.11	0.09	0.40	0.75	0.69	0.83
Al_2O_3	32.17	30.79	31.27	32.40	31.95	31.98	32.58	32.08
Cr_2O_3	0.16	< d.l.	0.07	0.01	0.02	< d.l.	0.01	< d.l.
Fe_2O_3*	0.98	1.17	1.38	0.36	0.22	1.03	0.35	0.33
CaO	17.97	17.72	17.36	17.81	18.09	18.12	17.96	17.60
total	90.15	88.04	88.35	89.00	88.79	90.15	89.96	89.22
cations								
Si	2.00	1.99	2.01	2.00	1.99	2.00	1.98	2.00
Ti	0.01	0.03	------	------	0.02	------	0.03	0.03
Al	1.96	1.93	1.94	1.99	1.97	2.02	1.98	1.97
Fe^{3+}	0.04	0.05	0.06	0.02	0.01	0.02	0.01	0.01
Ca	1.00	1.01	0.98	0.99	1.01	0.93	0.99	0.98
Fe^{2+}					0.02	0.01	0.04	0.02	0.01
XANES $Fe^{3+}/\Sigma Fe$	~1	~1	~1	~0.6	0.46	0.54	0.58	0.71

sample type: GM = grain mount; TS = thin section; TS-pt 1, 2, 3, 4 (see Fig. 3f for point locations)
< d.l. = less than detection limit
cations calculated on 8 oxygen basis
Fe_2O_3*: Fe first assumed to be entirely Fe^{3+} for cation calculations; for comparison, cations calculated with an all-Fe^{2+} assumption are also shown. Neither is correct (see XANES $Fe^{3+}/\Sigma Fe$ values) but illustrate the values of the two end-member scenarios for reference.
MgO, MnO, SrO, Na_2O, and K_2O analysed and not detected, although NC19-159 lawsonite locally contains Sr-rich zones that were not analysed with XANES.

Table S2b: EPMA data: representative compositions for epidote group minerals analysed by XANES.

mineral	Ep	Czo	Zo
locality	unknown	Pakistan	unknown
sample	Bayreuth xtal 3	Gilgit xtal 2	UMN xtal 1
type/pt	*GM*	*GM*	*GM*
SiO_2	35.20	36.66	37.56
TiO_2	0.14	0.10	0.08
Al_2O_3	24.17	29.36	33.34
Cr_2O_3	< d.l.	0.04	0.03
Fe_2O_3*	11.36	5.75	1.53
MnO	0.30	0.02	0.02
MgO	0.03	0.05	0.05
CaO	23.99	24.65	24.65
SrO	< d.l.	0.13	0.13
Na_2O	< d.l.	0.01	0.01
total	95.19	96.77	97.40
cations			
Si	2.96	2.92	2.90
Ti	0.01	0.01	-----
Al	2.39	2.76	3.03
Cr	-----	-----	-----
Fe^{3+}	0.80	0.38	0.10
Mn	0.02	0.01	-----
Mg	------	0.01	0.01
Ca	2.16	2.10	2.04
Sr	------	0.01	0.01
Na	------	-----	-----
X_{Fe}	0.25	0.12	0.03

sample type: GM = grain mount
< d.l. = less than detection limit
Fe_2O_3*: Fe assumed to be Fe^{3+} for cation calculations
K_2O < detection limit
cations calculated on 12.5 oxygen basis

$X_{Fe} = Fe^{3+}/(Al + Cr + Fe^{3+})$

3. EBSD methods and results

For the EBSD analysis, polished samples underwent an additional polishing step with colloidal silica (40 nm grain size) in order to remove intracrystalline damage due to previous polishing. Samples were also coated with a layer of 2-3 nm of amorphous carbon for electrical conduction.

Bayreuth

A Zeiss (formerly Leo) Gemini 1530 SEM with a Schottky emitter was used with an accelerating voltage of 20 keV and a beam current of about 2 nA to generate EBSD patterns from different slices of single crystals of lawsonite (Lws), clinozoisite (Czo), zoisite (Zo), and epidote (Ep). The diffraction patterns were recorded online with a Nordlys low-light camera with 4x4 pixel averaging and after image processing were analyzed with the Aztec program package (both from Oxford Instruments). Patterns were indexed with respective phases from the ICSD data base. Indexing was achieved with 7 to 11 bands yielding a mean angular deviation of 0.38 to 0.6° (Table); the orientation of each grain analyzed by XANES is shown in pole figures.

Table S3a: EBSD-derived orientation data for lawsonite, clinozoisite, zoisite and epidote single crystals (grain mounts); phi1, PHI and phi2 are Euler angles in the Bunge convention (Bunge 1982); a,b denote twin orientations in one grain; MAD stands for the mean angular deviation between the experimentally determined (# bands) and the calculated diffraction bands.

Mineral	phi1 [°]	PHI [°]	phi2 [°]	# bands	MAD [°]
Lws (UMN) xtal 2	57.08	86.75	76.51	10	0.59
Lws (UMN) xtal 3	154.27	26.72	0.17	10	0.49
Czo (Gilgit) xtal 1a	246.58	103.19	273.58	11	0.23
Czo (Gilgit) xtal 1b	246.15	102.67	92.05	8	0.43
Czo (Gilgit) xtal 2a	353.77	170.75	264.16	7	0.26
Czo (Gilgit) xtal 2b	171.63	9.76	277.94	8	0.43
Czo (Gilgit) xtal 3	88.69	87.95	358.16	9	0.12
Zo (unknown) xtal 1	94.56	39.16	79.58	11	0.49
Zo (unknown) xtal 2	82.28	91.81	89.27	11	0.38
Zo (unknown) xtal 3	81.79	89.53	156.27	8	0.38
Zo (unknown) xtal 4	77.19	171.26	82.48	10	0.60
Ep (Bayreuth) xtal 1	132.83	92.77	359.54	8	0.23
Ep (Bayreuth) xtal 3	98.75	24.96	96.28	7	0.36

Reference:
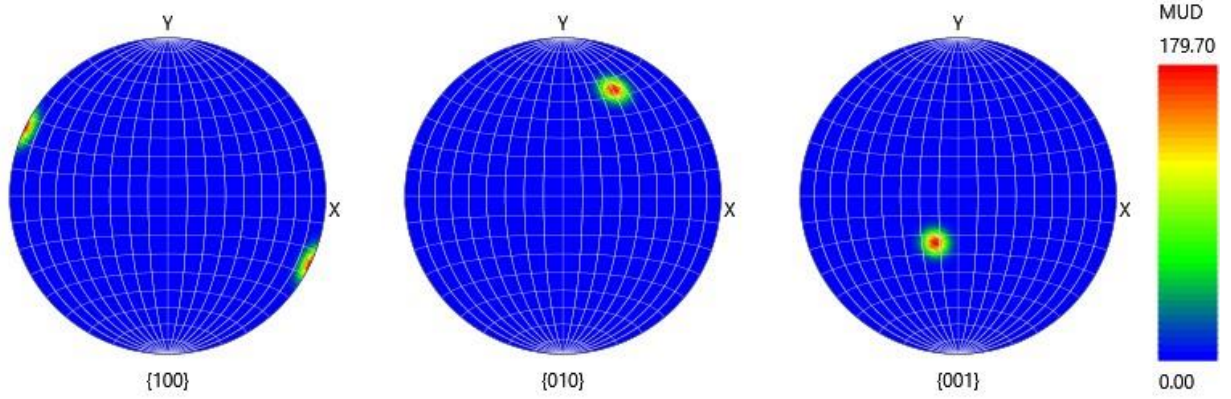Bunge, H.-J. (1982) Texture Analysis in Materials Science. London, Butterworths, 595 p.

Figure S3: Pole figures showing orientation of crystals analysed by EBSD. Crystal umbers refer to specific slices of single crystals in grain mounts.
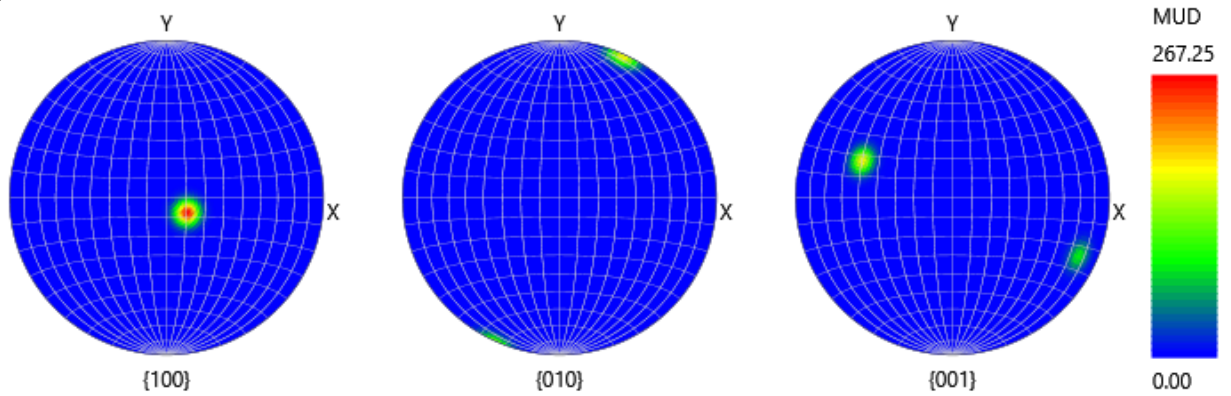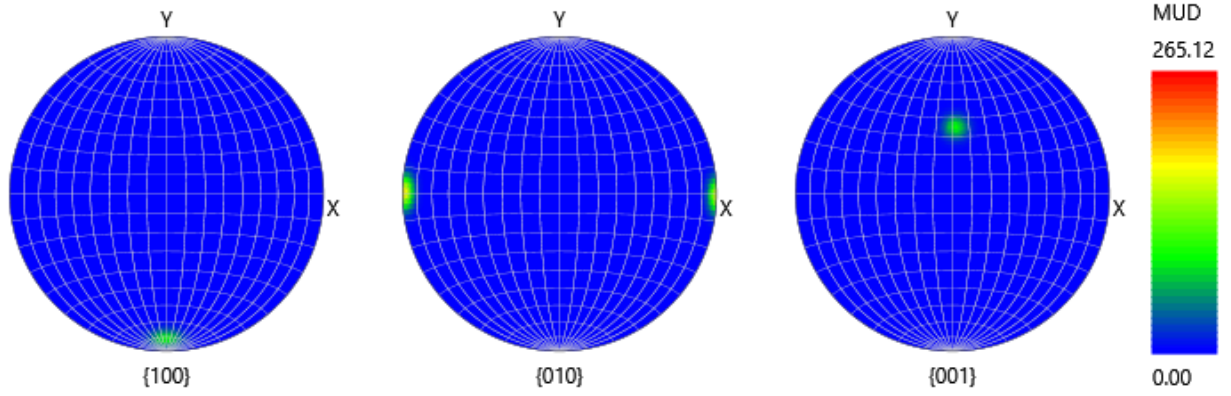
lawsonite (Franciscan, UMN collection)

crystal 2

{100} {010} {001}

crystal 3

{100} {010} {001}
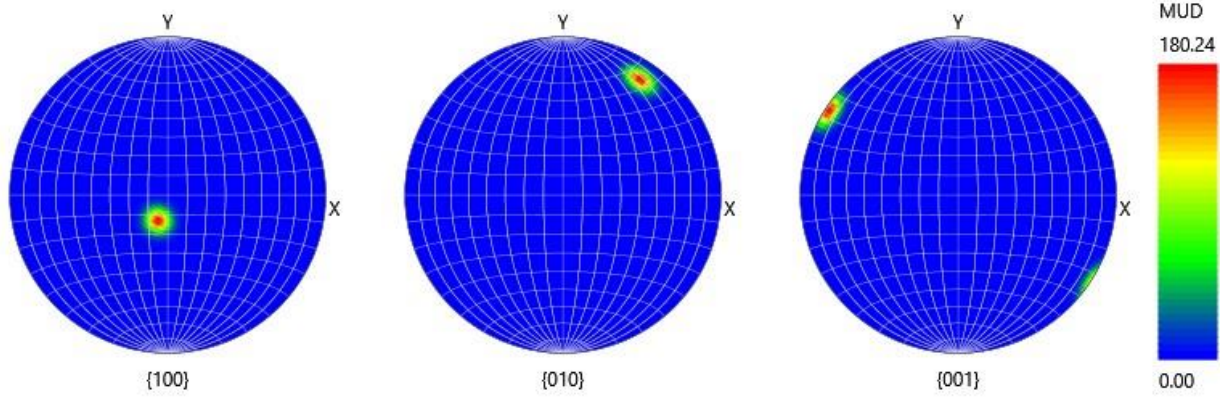
clinozoisite (Gilgit, Pakistan)

crystal 1

{100} {010} {001}

crystal 2

{100}   {010}   {001}

crystal 3

{100}   {010}   {001}
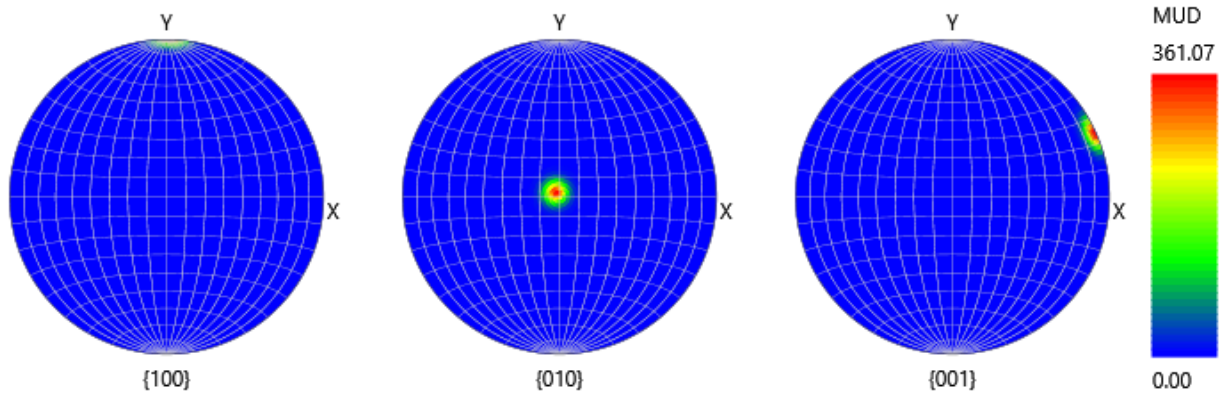
zoisite (unknown locality, UMN collection)

crystal 1

{100}   {010}   {001}

crystal 2

{100}   {010}   {001}

crystal 3

{100}   {010}   {001}

crystal 4

{100}   {010}   {001}
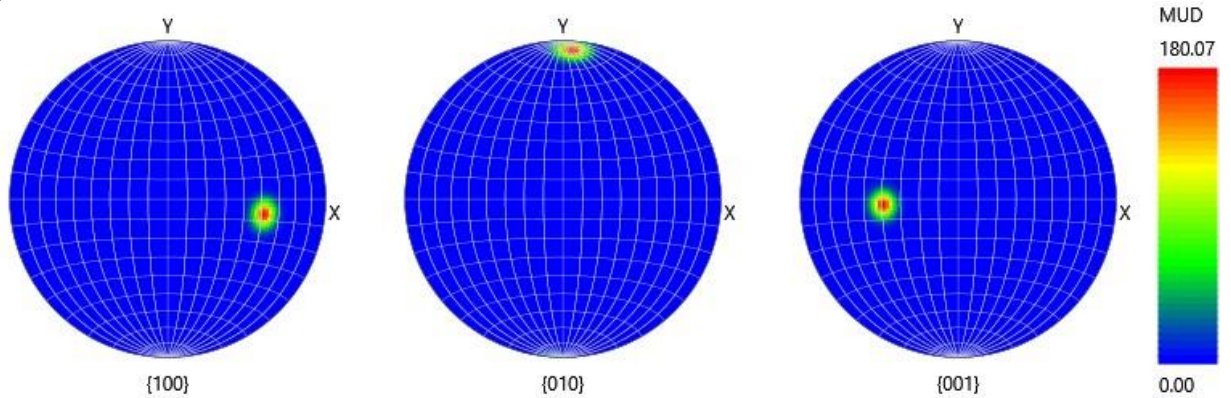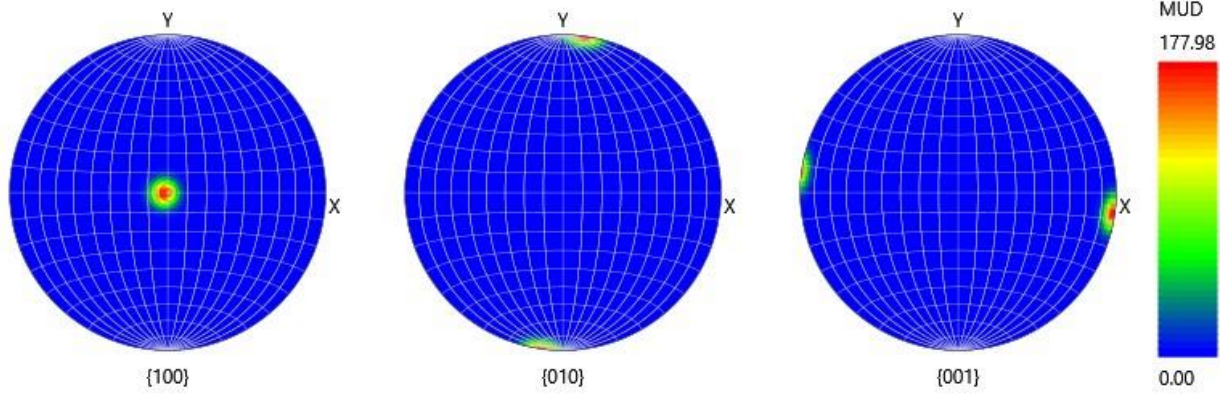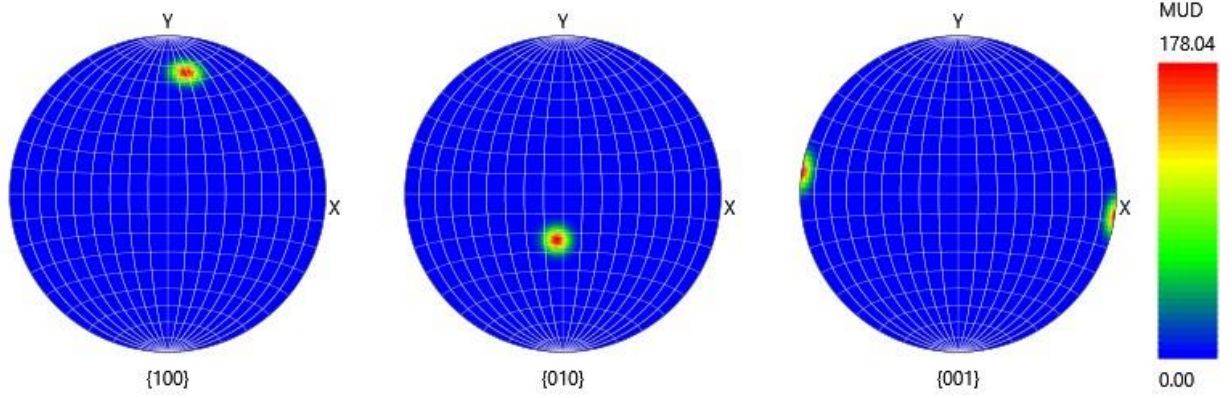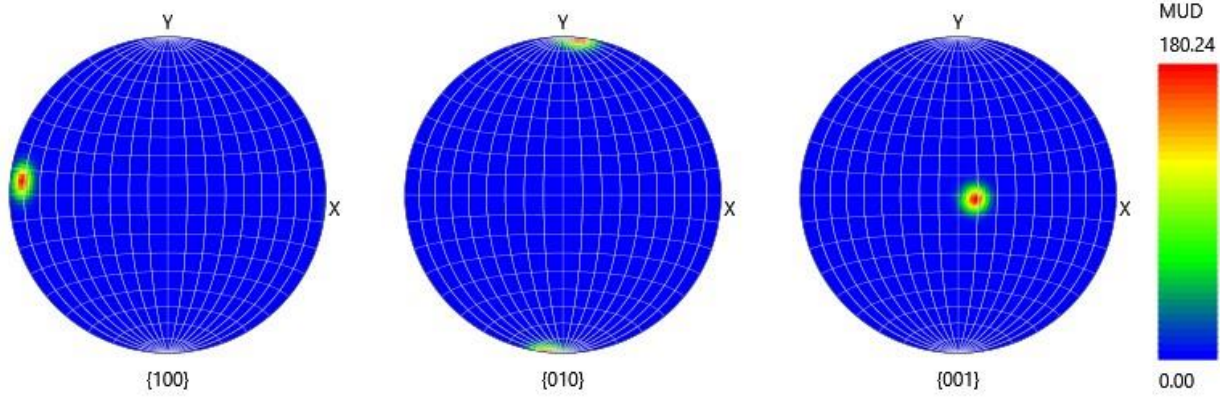
epidote (Bayreuth)

crystal 1
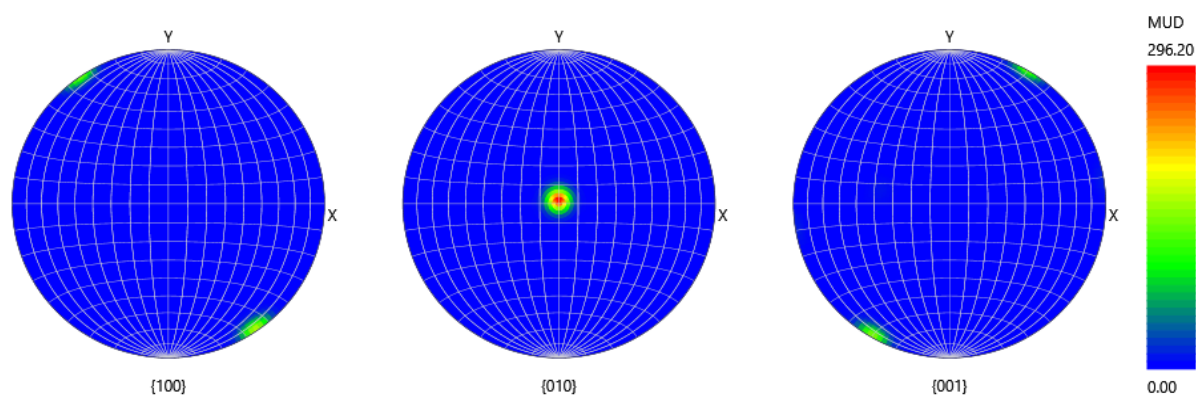
crystal 3
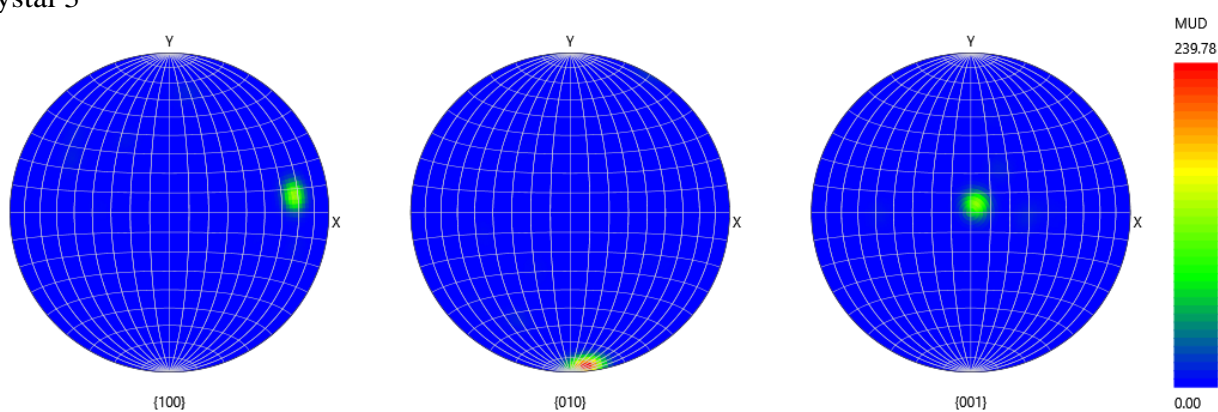
University of Minnesota

A Thermo Apreo 2S Lo-Vac SEM was used with an accelerating voltage of 20 keV to generate EBSD patterns from three slices of a single lawsonite crystal (Smithsonian, sample C3247). The diffraction patterns were analyzed with the Aztec program package from Oxford Instruments. Patterns were indexed with respective phases from the ICSD data base. Indexing parameters for each grain are given below, with pole figures showing the orientation of each analyzed grain/crystal.

Table S3b EBSD-derived orientation data for 3 distinct slices of a large lawsonite single crystal (Franciscan).

| Phase Name	Phase Fraction (%)	Phase Count	Mean Band Contr.	St. Dev. Band Contr.	Min Band Contr.	Max Band Contr.	Mean MAD	St. Dev. MAD	Min MAD	Max MAD
Lawsonite xtal 1	84.27	659	100.00	11.59	64.00	129.00	0.76	0.21	0.20	1.90
Zero Solutions	15.73	123	91.08	20.17	0.00	230.00				

Phase Name	Phase Fraction (%)	Phase Count	Mean Band Contr.	St. Dev. Band Contr.	Min Band Contr.	Max Band Contr.	Mean MAD	St. Dev. MAD	Min MAD	Max MAD
Lawsonite xtal 2	88.62	693	86.56	7.81	60.00	118.00	0.75	0.19	0.23	1.99
Zero Solutions	11.38	89	78.96	10.81	0.00	100.00				

Phase Name	Phase Fraction (%)	Phase Count	Mean Band Contr.	St. Dev. Band Contr.	Min Band Contr.	Max Band Contr.	Mean MAD	St. Dev. MAD	Min MAD	Max MAD
Lawsonite xtal 3	50.90	398	106.05	10.94	70.00	139.00	0.91	0.24	0.44	1.98
Zero Solutions	49.10	384	98.74	13.20	0.00	168.00				

lawsonite Smithsonian (C3247)

crystal 1

crystal 2

17

crystal 3

{100} {010} {001}

MUD
131.71

0.00
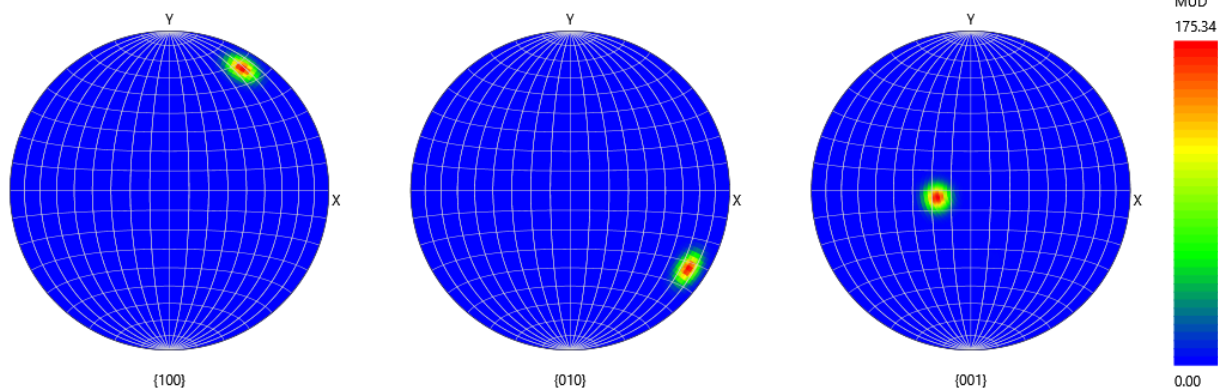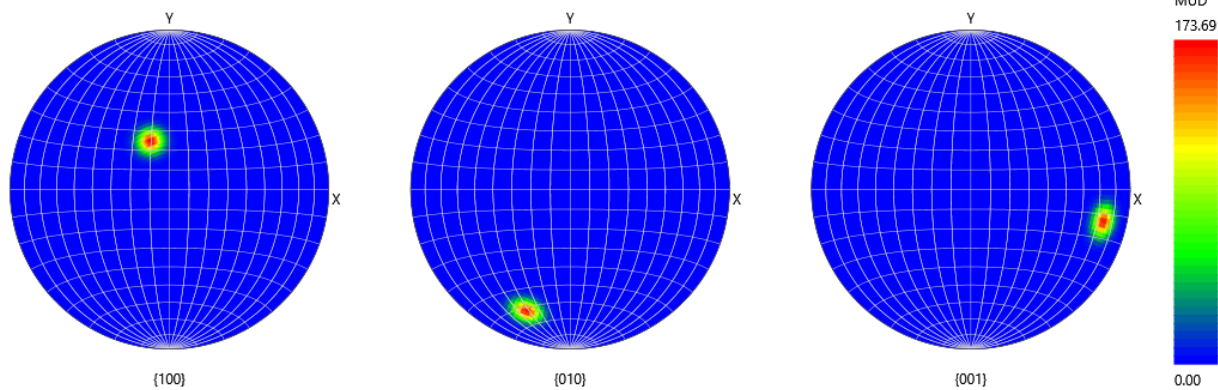
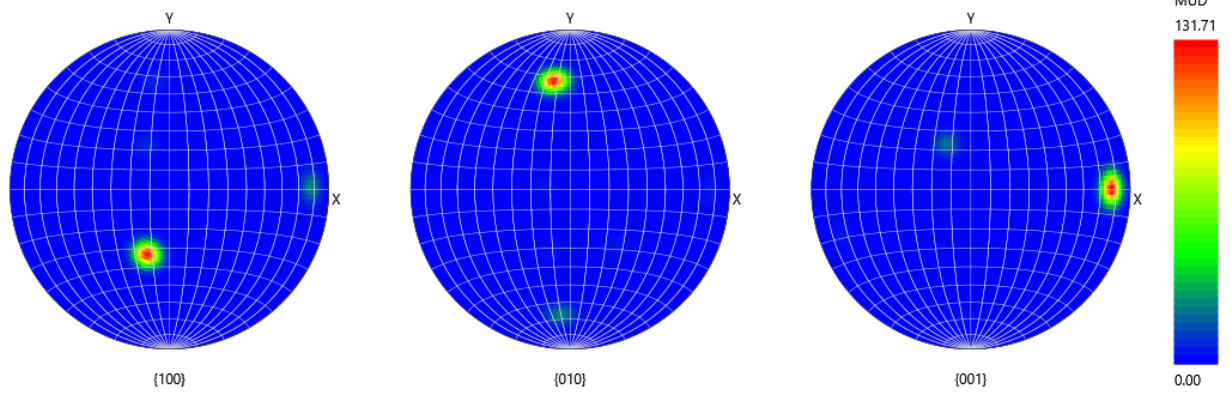## 4. Crystal structure models

Figure S4: Crystal structures of epidote, zoisite, and lawsonite. Images were created with CrystalMaker software.